

Predicting the Influence of Nanoformulations on Biomolecule Functionalities Using Machine Learning and ¹³C NMR Spectroscopy Data Derived from SMILES: A Case Study on Human Dopamine D1 Receptor Antagonists

Mariya L. Ivanova^{1,*}, [ORCID](#), Nicola Russo¹, [ORCID](#) and Konstantin Nikolic¹, [ORCID](#)

Author affiliations

¹School of Computing and Engineering, University of West London, London, UK

*Corresponding author mariya.ivanova@uwl.ac.uk

Abstract

This study contributes to ongoing research that aims to overcome challenges in predicting the bioapplicability of nanoformulations. It incorporates machine learning and ¹³C NMR spectroscopy data. In order to demonstrate the approach, from the PubChem world's largest publicly available chemical database, a bioassay on human dopamine D1 receptor antagonists was downloaded. From the mentioned bioassay the SMILES of compounds were extracted and converted into spectroscopy data by designed for this purpose software. The resulting data was then used for data preprocessing and machine learning, employing scikit-learn algorithms. The ML models were trained by 27,756 samples and tested by 5,466. From the estimators K-Nearest neighbour, Decision Tree Classifier, Random Forest Classifier, Gradient Boosting Classifier, XGBoosting Classifier and Support Vector Classifier, the last performed the best, achieving 71.5 % accuracy, 77.4 % precision, 60.6% recall, 68 % F1, 71.5 % ROC and 0.749 cross-validation score with 0.005 standard deviation. The methodology was designed to be versatile and capable of predicting any functionality of any compound, with or without added nanoformulations, when the appropriate data is available. In addition to the study presented in the article, the time- and cost-efficient CID-SID ML model was developed, giving an opportunity for researchers who have developed a compound and have obtained its PubChem CID and SID to check whether this compound is also a human dopamine D1 receptor antagonist. The metrics of CID_SID ML model were 80.2% accuracy, 86.3% precision, 70.4% recall, 77.6% F1, 79.9% ROC, five-fold cross-validation score 0.8071 with 0.0047 Standard deviation.

Key words: machine learning, ¹³C NMR spectroscopy, human dopamine D1 receptor antagonist, CID-SID ML model.

Introduction.

Bio-applicable nanoformulations (NFs) are structures at the nanoscale designed to assist biomolecules in different aspects, such as drug delivery, tissue engineering, theragnostic, imaging, sensing, vaccine development and a variety of nanodevices for medical purposes. This incorporation of nanotechnology and medicine created so-called nanomedicine. Although it is a relatively new domain, nanomedicine has already achieved significant results. Since the approval of the first nanotherapeutic in 1995 ([FDA, n.d.](#)), currently, around 100 more have been

approved by the Food and Drug Administration (FDA) and the European Medicines Agency (EMA) ([Shan et al., 2022](#)). However, the development of NFs for medical purposes is challenging because it cannot be based solely on conventional approaches used so far in healthcare. This is due to a variety of reasons, such as the materials are so small that a standard light microscope cannot adequately analyse the signals ([Ponta, 2024](#)); their dimensions are close to the quantum range, which, in turn, can change their properties ([Altammar, 2023](#)); Brownian forces influence particles up to one micron in size which effect increases with decreasing nanoparticle size, so directing particle motion is challenging ([Jin et al., 2017](#)).

Moreover, different methods for particle sizing provide dissimilar results ([Eitel, Bryant and Schope, 2021](#)), so their accurate sizing is relevant. In addition, the human serum (HS) could lead to changes in the size and surface potential of NFs, which occurs due to the absorption of albumin and/or the aggregation of fibrinogen by the functionalised and/or loaded NFs ([Fornaguera et al., 2015](#)). With ultrafast laser spectroscopy, researchers observed a size-dependent transition in the electronic properties of gold nanomaterials (NFs), ranging from metallic to transitional and then to non-metallic states ([Zhou et al., 2016](#)). This highlights the crucial role of size in determining the physical and chemical properties of NFs, including their conductance. Furthermore, studies have shown that even NFs with similar sizes and atom counts can exhibit significant variations in their toxicity ([Singh et al., 2020](#)). This emphasises the importance of considering factors beyond size, such as surface chemistry and structural defects, when assessing the properties and potential impacts of NFs.

The computer-based tool Quantitative Structure-Activity Relationship (QSAR), whose task is to predict the biological activity of chemical compounds based on their molecular structure, was used to address the unique properties of NFs, and nano-QSAR models addressing the unique properties of NFs were developed. However, their predictive power remains limited and under development ([Li et al. 2022](#)). Beyond nano-QSAR is the Structure and Activity Prediction Network (SAPNet) that aims to guide NF design by identifying crucial structural features for desired properties, but further refinement is necessary ([Rybińska-Fryca, Mikołajczyk and Puzyn, 2020](#)). A successful technique develops prediction implementing so-called quasi-simplified molecular input-line entry system (quasi-SMILES). Unlike the traditional SMILES line notation, which represents only the chemical structure of the compound, the quasi-SMILES notations contain all available relevant electrical data ([Toropova and Toparov, 2024](#)). Moreover, imaging modality has been explored for predicting nanoformulations, and the approach has been successfully applied in cancer research ([Cooley, Wegierak and Exner, 2024](#)).

The concerns regarding the NFs applications are the cytotoxicity that can impair or kill cells; genotoxicity that can damage the DNA; immunogenicity that can trigger inflammation, allergies or autoimmune disorder; accumulations in unintended organs; long-time side effects; the direct influence over the biomolecule functionality by the assisting NF. Herein, the study explored particularly, the last concern. For this purpose, the information that can be provided by ^{13}C NMR spectroscopy and the prediction power of machine learning (ML) were incorporated. NMR spectroscopy measures the atomic nuclei's absorption and emission of radiofrequency radiation. The ^{13}C NMR spectroscopy technology utilizes the magnetic property of the ^{13}C isotope ([Felli and Pierattelli, 2022](#)). The ^{13}C nucleus contains six protons and seven neutrons. The extra

$\frac{1}{2}$ spin makes the ^{13}C isotope behave as a little magnet. As a result, NMR spectroscopy is sensitive to differences in the chemical structure of the organic molecule, giving information for the connectivity and relative position of the carbon atoms in the molecule. The hypothesis is that the presence of NF would affect the environment of the carbon atoms in the carbon skeleton of the biomolecules ([Abramson et al., 2024](#)) and respectively this will be detected by ^{13}C NMR spectroscopy and used by ML for predicting the effect which NF caused.

A variety of studies have been conducted exploring the incorporation of ML and ^{13}C NMR spectroscopy, such as Džeroski et al. ([1997](#)) exploring the correlations between peak patterns and chemical structure using machine learning; Xu, Zhou and Hong ([2024](#)) providing establishment of a correspondence between the molecular graphs and NMR spectra; Williamson et al. ([2024](#)) predicting ^{13}C NMR chemical shifts with message passing neural network (MPNN); Duprat et al. ([2024](#)) detecting chemical shifts of Benzenic compounds; CASPRE ([n.d.](#)) software predicting ^{13}C spectroscopy data by uploading SMILES, International Chemical Identifier (inChI) or drawing the structure of the compound; Rigel, Li and Brüscheweiler ([2024](#)) predicting NMR spectra with COLMARppm software using NMR data obtained in an aqueous solution; Meiler and Will ([2002](#)) using artificial neural network (ANN) to generate new structures based on information obtained by ^{13}C NMR.

The hypothesis was demonstrated using a PubChem bioassay of quantitative High-throughput screening (qHTS) on human dopamine D1 receptor antagonists ([NIH, 2011](#)). The bioassay contained 359,035 rows of compound records and 10 columns with the features of these compounds. This bioassay aimed to select and develop allosteric modulators of the dopamine D1 receptor for in vivo and in vitro applications. It was performed by measuring the compound dopamine D1 receptor antagonism with an EC80 addition of dopamine by tracking calcium flux in a force-coupled inducible Hek293 Trex D1 cell line. The compound concentration utilized in this bioassay was 10.0microM. For more information regarding the bioassay protocol, please refer to the bioassay documentation ([NIH, 2011](#)). For the purpose of the study from this bioassay ([NIH, 2011](#)), the canonical SMILES line notations of the compounds were extracted and converted into ^{13}C NMR spectroscopy data by the NMRDB software ([n.d.](#)). The energy data obtained in this way was used for developing ML models that can predict whether the compound is an antagonist of the human dopamine D1 receptor. The influence of an NF over the functionality of this structure is expected to be detectable by this approach as well.

ML is increasingly integrated into drug development, driven by the search for innovative approaches that can significantly reduce the time and cost of research ([Turzo, Hantz, Lindert, 2022](#); [Ivanova, Russo and Nikolic, 2024](#); [Dara et al., 2022](#)). Regarding the dopamine D1 receptor antagonists classification has been conducted using topological descriptors ([Kim et al., 2006](#)); effective identification of novel agonists of dopamine receptors has been obtained using predictive or generative geometric ML ([Sobodu et al., 2024](#)); agonists and antagonists have been predicted, using topological fragment spectra (TFS)-based support vector machine (SVM), ([Fujishima et al., 2007](#)). However, the approach presented in the current article has not been reported in the available literature.

The approach utilised in the study is explained in the section Methodology below and illustrated in Fig. 1.

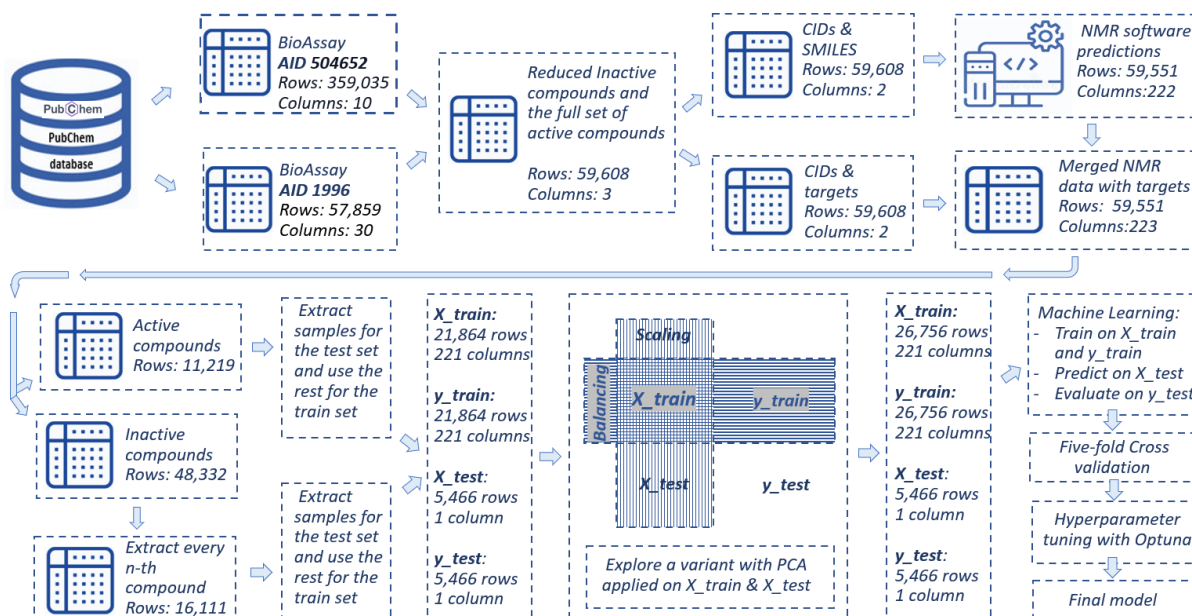


Fig. 1.

¹³C NMR spectroscopy data-based ML model for predicting of human dopamine D1receptor antagonists' methodology

Out of the scope of the study, but for the benefit of the researchers interested in the human dopamine D1 receptor antagonists, the CID-SID ML model (Ivanova, Russo and Nikolic,2025) was developed. This ML model can predict the functionality of a compound based on the information encoded into its PubChem CID and SID and thus assists drug researchers with a cost and time-efficient tool for the early stage of drug development. The generated code is provided on GitHub for direct usage by the interested.

Methodology

From the provided by PubChem bioassay AID 504652 (NIH, 2011), the columns with SMILES notations, outputs of the screening and CIDs of the compounds were extracted. The resulting dataset was then merged with the water solubility dataset PubChem AID 1996 (NIH, 2010), keeping only the unique identifiers (CIDs) of the substances for both datasets. This reduced the inactive compounds to some extent. Then, the reduced inactive compounds were concatenated with all active compounds from the PubChem bioassay AID 504652 (NIH, 2011). The newly formed dataset was used to create two datasets, as the one contained the CIDs and SMILES notations of the compounds and the other the CIDs and the relevant outputs from the screening, which later were used as targets.

The SMILES strings from the former dataset were used for calculating the ^{13}C NMR spectroscopy by the software NMRDB ([n.d.](#)). From the list of signals, i.e. spectroscopy picks predicted by the software, the number of picks per diapason was counted. The length of the diapasons was defined by integers. From this data, a data frame was created that was merged with the target data frame (the second dataset mentioned above, which contained the compounds` CIDs and screening outputs, i.e. the targets). Thus, a data frame with ^{13}C spectroscopy information and targets was obtained. The inactive compounds of this data frame then were additionally reduced, remaining only every third inactive compound. Hence, the final data frame necessary for ML was completed. From it, an equal number of samples were extracted for each target and created the test sets. The rest of the samples formed the train sets. Further, the datasets were scaled, and the train sets were balanced, as illustrated in Fig.1. Scaling brought features to a similar scale, preventing feature domination and eliminating the issue that can occur due to vast differences in feature ranges ([Ahsan et al., 2021](#)) while the balancing ensures that the ML model will learn from both classes effectively ([Gnip, Vokorokos and Drotár, 2021](#)) Both processes enhance the accuracy of the ML models. The ML binary classification estimators used in the study were: K-Nearest neighbour (KNN) ([Cunningham and Delany, 2021](#)), Random Forest Classifier (RFC) ([Manzali and Elfar, 2023](#)), XGBoosting Classifier (XGBC) ([Bentéjac, Csörgő and Martínez-Muñoz, 2021](#)), Decision Tree Classifier (DTC) ([Klusowski and Tian, 2024](#)), Gradient Boosting Classifier (GBC) ([Mushava and Murray, 2024](#)) and Support Vector Classifier (SVC) ([Guido et al., 2024](#)). Principle component analysis (PCA) was used to reduce the high dimensionality of the dataset that occurs due to the conversion of SMILES notations into spectroscopy data. The number of components suitable for the given dataset was calculated using unsupervised ML, and subsequently, the suggested number of components was applied for PCA dimensionality reduction.

Metrics suitable for binary classification (Rainio, Teuho and Klén, 2024) were used to evaluate the ML models. They were as follows:

- (i) Accuracy was calculated by dividing the correct prediction by the total number of predictions, unveiling the overall correctness of the ML model.
- (ii) Precision exposes how many of the positive predictions are true positive
- (iii) Recall reveals how many of the positive cases in the data set have been identified correctly
- (iv) F1-score is the harmonic mean of the precision and the recall
- (v) ROC curves illustrate how a binary classifier's performance changes as its decision threshold for classifying instances varies.

Due to the size of the dataset, hyperparameter tuning ([Panda, 2019](#)) would take a long time. To reduce the time without making quality compromises, from the final dataset, a representative dataset of 1000 compounds was extracted and used for hyperparameter tuning performed by Optuna ([Akiba et al., 2019](#)). The hyperparameters considered during the hyperparameter tuning were as follows:

- (i) The 'rbf' kernel (radial basis function kernel) finds boundaries and achieves high accuracy by mapping data into a higher-dimensional space, separating non-linearly

- separable data; the kernel 'linear' - the choice of the SVM when the data can be effectively separated by a linear boundary.
- (ii) The parameter C minimises the training error, controlling the balance between the closest data points and the separating hyperplane.
 - (iii) Gamma, which controls the influence of a single training example

The difference between the train and test accuracy was traced because it provided information about the presence of overfitting, i.e. when the model performs well on the train set but not on unseen data. This scrutinising for overfitting was the last step before the final model was selected and visualised by plotting the learning curve, matrix and area under the curve (AUC).

Results and discussion

From the above-listed ML classifiers, SVC was the most suitable for the study. It obtained 71.5% accuracy, 77.4% precision, 60.6% recall, 68% F1 and 71.5% ROC, followed by XGBC with Accuracy 68.8% accuracy, 73.7% precision, 58.7 % recall, 65.3% F1 and ROC 68.8% ROC ([Table ESM 1](#)). The mean cross-validation ordered the classifiers in the same order where the cross-validation score of SVC based on accuracy was 0.7487 with 0.003 standard deviations for SVC and 0.7207 with 0.0054 standard deviations for XGBC, i.e. the SVC model across the data set obtained mean 74.87% accuracy and for XGBC the accuracy was 72.07% ([Table ESM 2](#)). The five-fold cross-validation results were higher than the ML model results and since the difference between them was less than 5%, this indicated that the model generalized well.

The hyperparameter tuning with Optuna suggested kernel='rbf', C=493.2744094205687, gamma = 0.00040591543979010816. However, the model performed with these values obtained 68.51% accuracy, which is lower than the accuracy performed with the default set of values, i.e. kernel='rbf', C=1, gamma = 'scale', where the value 'scale' means that the algorithm automatically will define the best reasonable initial value for gamma. This hyperparameter is calculated by number of features in the dataset multiply by the variance of the features in the dataset.

Regarding the usage of PCA, unsupervised learning suggested the number of components to be reduced from 221 to 23. However, the dimensionality reduction with PCA with 23 components did not improve the performance of the ML model. The SVC achieved 64.1% accuracy, 68.6% precision, 51.8 % recall, 59.1% F1 and 64.1% ROC, followed by RFC with 61.9% accuracy, 70.4% precision, 41.1 % recall, 51.9% F1, 61.9% ROC ([Table ESM 4](#)). The five-fold cross-validation score of SVC was 0.683 with 0.0052 standard deviations, followed by RFC with 0.6713 cross-validation score and 0.0072 standard deviations ([Table ESM 5](#)). Visualisation of the SVC model is illustrated in [Fig ESM 4](#). Learning curve; [Fig. ESM 5](#). AUC; [Fig. ESM 6](#). Confusion matrix; [Table ESM 6](#). Classification report.

So, the final ML model chosen in the study was SVC with default hyperparameters that achieved 71.5% Accuracy, 77.4% Precision, 60.6% Recall, 68% F1, 71.5% ROC and cross-validation score 0.749 with 0.0036 standard deviations. The final model was visualised with the learning curve([Fig. ESM 1](#)), AUC ([Fig. ESM 2](#)), matrix ([Fig. ESM 3](#)) and classification report ([Table ESM 3](#)).

The CID_SID ML model ([Ivanova, Russo and Nikolic, 2025](#)), which was not a primary object of exploration in the presented study, was developed in favour of the researchers interested in human dopamine D1 receptor antagonists. The best-presented estimator was XGBC achieving Accuracy 80.2%, Precision 86.3%, Recall 70.4%, F1 77.6%, ROC 79.9% ([Table ESM 7](#)) and cross-validation score 0.8071 with 0.0047 Standard deviation ([Table ESM 8](#)), followed by GBC with Accuracy 80.1%, Precision 88.5%, Recall 67.7%, F1 76.7%, ROC 79.7% ([Table ESM 7](#)), and a five-fold cross-validation score 0.8031 with 0.0038 standard deviation ([Table ESM 8](#)). Thus, a drug developer can check if their compound is also a human dopamine D1 receptor antagonist using only its PubChem CID and SID. Given the methodology requirements ([Ivanova, Russo and Nikolic, 2025](#)), the dataset contained only CIDs, SIDs and targets of the considered compounds. The CID_SID ML model was trained with 19,438 samples and tested with 4,723. Standardisation of data was processed by scikit-learn standard scalar function, which transformed data so that each feature has a mean of 0 and a standard deviation of 1, preventing the occurrence of feature prioritising. Balancing of train data was performed with a random over sampler approach randomly selecting instances from the target 1 and creating duplicates of them in order to handle the imbalanced dataset. The ML model was hyperparameter tuned by grid search, and the resulting hyperparameter values were as follows:

- (i) `colsample_bytree=1.0` (that randomly selects a subset of features for each tree, reducing the correlation between trees in the ensemble and thus preventing overfitting and improving the generalisation)
- (ii) `learning_rate = 0.1` (determine how much the model's parameters are adjusted during each iteration of the training process)
- (iii) `max_depth=5` (limits the number of levels or nodes the model has from the root node to the leaf nodes)
- (iv) `min_child_weight=5` (control the minimum number of samples required to create a new node in a tree)
- (v) `n_estimators=200` (denotes the number of decision trees within SVC)
- (vi) `subsamples=0.9` (It controls the fraction of training data randomly sampled for each tree in the ensemble)

Tracing the deviation between test and train accuracy was performed, and it was found that the overfitting started for `max_depth > 12` where the test accuracy was 80%, revealing that the ML model was not overfitted ([Fig. ESM 7](#)). The final CID_SID ML model was visualised by plotting the learning curve ([Fig. ESM 8](#)), AUC ([Fig. ESM 9](#)), confusion matrix ([Fig. ESM 10](#)), and classification report ([Table ESM 9](#)).

Conclusion

Although the spectroscopy data used in the study was obtained by software developed for this purpose, the expectations are that the approach will be applicable when the data is obtained through actual ¹³C NMR spectroscopy technology. Although the ML model was developed primarily to handle the challenges related to predicting NFs for medical purposes, the presence of NF is not mandatory. The methodology can be applied for predicting any functionality of a biomolecule when the data necessary for ML meets the data generation requirements. The study

paved a path for further exploration for obtaining more precise ML models. The additionally developed CID_SID ML model can give an insight into whether a compound is a human dopamine D1 receptor antagonist based only on its PubChem CID and SID.

Author Contributions

MLI, NR and KN conceptualized the project and designed the methodology. MLI and NR wrote the code and processed the data. KN supervised the project. All authors were involved with the writing of the paper.

Funding

MLI thanks the UWL Vice-Chancellor's Scholarship Scheme for their generous support.

Acknowledge

We sincerely thank NIH for providing access to their PubChem database.

Data and Code Availability Statement

The raw data used in the study is available through the PubChem portal:

<https://pubchem.ncbi.nlm.nih.gov/>

The code generated during the research is available on GitHub:

https://github.com/articlesmli/13C_NMR_ML_model_D1.git

Conflicts of Interest

The authors declare no conflict of interest.

Footnotes

The article is dedicated to Luben Ivanov

References

- Abramson J, Adler J, Dunger J et al. (2024) Accurate structure prediction of biomolecular interactions with AlphaFold 3. *Nature* 630: 493–500. doi.org/10.1038/s41586-024-07487-w.
- Ahsan MM, Mahmud MAP, Saha PK, Gupta KD, Siddique Z (2021) Effect of Data Scaling Methods on Machine Learning Algorithms and Model Performance. *Technologies* 9(3): 52. doi.org/10.3390/technologies9030052
- Akiba T, Sano S, Yanase T, Ohta T and Koyama M (2019). Optuna: A Next-generation Hyperparameter Optimization Framework. In: The 25th ACM SIGKDD International Conference on Knowledge Discovery & Data Mining, pp. 2623-2631. DOI: 10.48550/arXiv.1907.10902
- Altammar KA (2023) A review on nanoparticles: characteristics, synthesis, applications, and challenges. *Frontier in Microbiology* 14:1155622. doi.10.3389/fmicb.2023.1155622
- Bentéjac C, Csörgő A and Martínez-Muñoz D (2021) A comparative analysis of gradient boosting algorithms. *Artificial Intelligence Review* 54: 1937–1967. doi.org/10.1007/s10462-020-09896-5
- CASPRES (n.d.) CASPRE - ¹³C NMR Predictor. Available at: <https://caspre.ca/> (accessed 14 Jan 2025)
- Cooley MB, Wegierak D and Exner A A (2024) Using imaging modalities to predict nanoparticle distribution and treatment efficacy in solid tumours: The growing role of ultrasound. *WIREs Nanomedicine and Nanobiotechnology* 16(2): e1957. doi.org/10.1002/wnan.1957
- Cunningham P and Delany SJ (2021) K-Nearest Neighbour Classifiers - A Tutorial. *ACM Computing Surveys* 54(6): Article 128 (July 2022), 25 pages. doi.org/10.1145/3459665
- Dara S, Dhamecherla S, Jadav SS, Babu CHM and Ahsan MJ (2022) Machine Learning in Drug Discovery: A Review. *Artificial Intelligence Review* 55:1947–1999. doi.org/10.1007/s10462-021-10058-4
- Duprat F, Ploix JL and Dreyfus G (2024) Can Graph Machines Accurately Estimate ¹³C NMR Chemical Shifts of Benzenic Compounds? *Molecules* 29(13): 3137. doi.org/10.3390/molecules29133137

Džeroski S, Schulze-Kremer S., Heidtke KR, Siems K and Wettschereck D (1997) Diterpene Structure Elucidation from ^{13}C NMR-Spectra with Machine Learning. In: Lavrač, N., Keravnou, E.T., Zupan, B. (eds) *Intelligent Data Analysis in Medicine and Pharmacology*. The Springer International Series in Engineering and Computer Science, vol 414. Springer, Boston, MA. doi.org/10.1007/978-1-4615-6059-3_12

Eitel K, Bryant G and Schöpe HJ (2020) A Hitchhiker's Guide to Particle Sizing Techniques. *Langmuir* 36 (35): 10307-10320. doi.org/10.1021/acs.langmuir.0c00709

FDA (n.d.) Doxorubicin HCl Release from Liposomal Doxorubicin Formulations Autonomous Capillary Electrophoretic (CE) In Vitro Release Test (IVRT) Method . Available at chrome www.fda.gov/media/168790/download#:~:text=In%201995%2C%20U.%20S.%20Food%20and,available%20in%20the%20U.S.%20market (accessed 14 Jan 2025)

Felli IC and Pierattelli R (2022) ^{13}C Direct Detected NMR for Challenging Systems. *Chemical Reviews* 122 (10): 9468-9496. doi.10.1021/acs.chemrev.1c00871.

Fornaguera C, Calderó G, Mitjans M, Vinardell MP, Solansa C and Vauthier C (2015) Interactions of PLGA nanoparticles with blood components: protein adsorption, coagulation, activation of the complement system and hemolysis studies. *Nonoscale* 14(7): 6045-6058. doi.org/10.1039/C5NR00733J

Fujishima S, Takahashi Y, Nishikori K, Katoh and Okada T (2007) Extended Study of the Classification of Dopamine Receptor Agonists and Antagonists using a TFS-based Support Vector Machine. *New Generation Computing*. 25: 203–212. doi.org/10.1007/s00354-007-0012-x

Furxhi I, Murphy F, Mullins M, Arvanitis A and Poland CA (2020) Practices and Trends of Machine Learning Application in Nanotoxicology, *Nanomaterials* (Basel, Switzerland) 10(1): 116. doi. org/10.3390/nano10010116.

Gnip P, Vokorokos L and Drotár P (2021) Selective oversampling approach for strongly imbalanced data. *PeerJ Computer Science* 18(7): e604. doi: 10.7717/peerj-cs.604

Guido R, Ferrisi S, Lofaro D and Conforti D (2024) An Overview on the Advancements of Support Vector Machine Models in Healthcare Applications: A Review. *Information*, 15(4): 235. doi.org/10.3390/info15040235

Ivanova ML, Russo N, Djaid N and Nikolic K (2024) Application of machine learning for predicting G9a inhibitors. *Digital Discovery* 3(10):2010-2018. doi.10.1039/d4dd00101j.

Ivanova ML, Russo N and Nikolic K (2025) Predicting novel pharmacological activities of compounds using PubChem IDs and machine learning (CID-SID ML model). *ArXiv*. doi.org/10.48550/arXiv.2501.02154

Jin H, Liu N, Ku X and Fan J (2017) Preferential frequency and size effect of the Brownian force acting on a nanoparticle. *Journal of Fluid Mechanics* 828: 648-660. doi:10.1017/jfm.2017.512

Kim H-J, Cho YS, Koh HY, Kong JY, No KT and Pae AN (2006) Classification of dopamine antagonists using functional feature hypothesis and topological descriptors. *Bioorganic & Medicinal Chemistry* 14(5):1454-1461. doi.org/10.1016/j.bmc.2005.09.072

Klusowski JM and Tian P M (2024) Large scale prediction with decision trees. *Journal of the American Statistical Association* 119(545): 525-537. doi.org/10.1080/01621459.2022.2126782

Li J, Wang C, Yue L, Chen F, Cao X and Wang Z (2022) Nano-QSAR modelling for predicting the cytotoxicity of metallic and metal oxide nanoparticles: A review, *Ecotoxicology and Environmental Safety* 243:113955. org/10.1016/j.ecoenv.2022.113955

Manzali Y and Elfar M (2023) Random Forest pruning techniques: a recent review. In *Operations research forum* 4 (2): 43. Cham: Springer International Publishing.

Meiler J and Will M (2002) Genius: A Genetic Algorithm for Automated Structure Elucidation from ¹³C NMR Spectra. *Journal of the American Chemical Society* 124 (9): 1868-1870. doi.10.1021/ja0109388.

Mushava J and Murray M (2024) Flexible loss functions for binary classification in gradient-boosted decision trees: An application to credit scoring. *Expert Systems with Applications* 238: 121876. doi.org/10.1016/j.eswa.2023.121876

NIH (2010) AID 1996 - Aqueous Solubility from MLSMR Stock Solutions. Available at: https://pubchem.ncbi.nlm.nih.gov/bioassay/1996_5 (accessed 14 Jan 2025)

NIH (2011) AID 504652 - Antagonist of Human D 1 Dopamine Receptor: qHTS – PubChem. Available at: <https://pubchem.ncbi.nlm.nih.gov/bioassay/504652> (accessed 14 Jan 2025)

NIH (2025) PubChem. Available at: <https://pubchem.ncbi.nlm.nih.gov/> (accessed 14 Jan 2025)

NMRDB (n.d.) Predict ¹³C NMR. Available at: <https://nmrdb.org/13c/index.shtml?v=v2.138.0> (accessed 14 Jan 2025)

Nozari H, Ghahremani-Nahr J and Szmelter-Jarosz A (2024) AI and machine learning for real-world problems. In Kim S and Deka GC (eds.) *Advances In Computers* 134: pp. 1-12. Elsevier. doi.org/10.1016/bs.adcom.2023.02.001.

Oloff S H (2005). *Development of computer aided drug discovery methods based on machine learning techniques and application to the dopamine D1 receptor*. PhD Thesis, The University of North Carolina at Chapel Hill.

Panda (2019) Hyperparameter tuning *Research Gate* doi: 10.13140/RG.2.2.11820.21128

Ponta A (2024) Considerations for Drug Products that Contain Nanomaterials. *FDA*. 15 May Available at: <https://www.fda.gov/drugs/cder-small-business-industry-assistance-sbia/considerations-drug-products-contain-nanomaterials#:~:text=FDA%20recently%20released%20the%20guidance,to%20conventional%20manufacture%20or%20storage> (accessed 10 January 2025)

Rainio O, Teuho J and Klén R (2024) Evaluation metrics and statistical tests for machine learning. *Scientific Reports* 14: 6086. doi.org/10.1038/s41598-024-56706-x

Rigel N, Li D-W and Brüsweiler R 2024 COLMARppm: A Web Server Tool for the Accurate and Rapid Prediction of ¹H and ¹³C NMR Chemical Shifts of Organic Molecules and Metabolites. *Analytical Chemistry* 96 (2): 701-70. doi.10.1021/acs.analchem.3c03677

Rybinska-Fryca A, Mikolajczyk A and Puzyn T (2020) Structure–activity prediction networks (SAPNets): a step beyond Nano-QSAR for effective implementation of the safe-by-design concept, *Nanoscale* 40(10): 20669-20676. doi.org/10.1039/D0NR05220E.

Shan X, Gong X, Li J, Wen J, Li Y, Zhang Z. Current approaches of nanomedicines in the market and various stage of clinical translation. *Acta Pharm Sin B*. 2022;12(7):3028–3048. doi: 10.1016/j.asb.2022.02.025.

Singh AV, Ansari MHD, Rosenkranz D, Maharjan RS, Kriegel FL, Gandhi K, Kanase A, Singh R, Laux P, Luch A (2020) Artificial Intelligence and Machine Learning in Computational Nanotoxicology: Unlocking and Empowering Nanomedicine. *Advanced Healthcare Materials*: 9(17): 1901862. doi.org/10.1002/adhm.201901862

Sobodu T, Yusuf A, Kiel D and Kong D (2024) Discrimination vs. Generation: The Machine Learning Dichotomy for Dopaminergic Hit Discovery. *ArXiv*. arxiv.org/pdf/2409.12495

Toropova AP and Toropov AA (2024) The coefficient of conformism of a correlative prediction (CCCP): Building up reliable nano-QSPRs/QSARs for endpoints of nanoparticles in different experimental conditions encoded via quasi-SMILES, *Science of The Total Environment* 927: 172119. doi.org/10.1016/j.scitotenv.2024.172119.

Turzo SBA, Hantz ER, Lindert S (2022) Applications of machine learning in computer-aided drug discovery. *QRB Discovery* 3:e14. doi:10.1017/qrd.2022.12

Williamson D, Ponte S, Iglesias I, Tonge N, Cobas C, Kemsley EK (2024) Chemical shift prediction in ¹³C NMR spectroscopy using ensembles of message passing neural networks (MPNNs). *Journal of Magnetic Resonance* 368:107795. doi.org/10.1016/j.jmr.2024.107795.

Xu H, Zhou Z and Hong P (2024) Enhancing Peak Assignment in ¹³C NMR Spectroscopy: A Novel Approach Using Multimodal Alignment. ArXiv. doi.org/10.48550/arXiv.2311.13817.

Yamada A (2022) Computational Analyses of Plasmonics of a Silver Nanoparticle in a Vacuum and in a Water Solution by Classical Electronic and Molecular Dynamics Simulations. *Physical Chemistry*. 126: 4762-4771. doi.org/10.1021/acs.jpca.2c02811.

Zhou M, Zeng C, Chen Y, Zhao S, Sfeir MY, Zhu M and Jin R (2016) Evolution from the plasmon to exciton state in ligand-protected atomically precise gold nanoparticles. *Nature Communications* 7(10): 13240. doi.org/10.1038/ncomms13240

Electronic Supplementary material

1. Tables

Table ESM 1. Results of ML with ^{13}C NMR data of human dopamine D1 receptor antagonists.

	1.Algorithm	2.Accuracy	3.Precision	4.Recall	5.F1	6.ROC
0	SVM	0.715	0.774	0.606	0.680	0.715
4	XGBoost	0.688	0.737	0.587	0.653	0.688
2	RandomForest	0.653	0.792	0.416	0.546	0.653
3	GradientBoost	0.650	0.674	0.582	0.625	0.650
5	K-nearest	0.612	0.671	0.441	0.532	0.612
1	Decision	0.578	0.596	0.483	0.534	0.578

Table ESM 2. Five-fold cross-validation results of ML with ^{13}C NMR data of human dopamine D1 receptor antagonists.

	1.Algorithm	2.Mean CV Score	3.Standard Deviation	4.List of CV Scores
0	SVM	0.7487	0.0030	[0.7508, 0.7461, 0.7536, 0.7472, 0.7461]
4	XGBoost	0.7207	0.0054	[0.7252, 0.7144, 0.7236, 0.7265, 0.7141]
2	RandomForest	0.7073	0.0021	[0.7065, 0.7084, 0.7102, 0.7073, 0.704]
3	GradientBoost	0.6885	0.0048	[0.6925, 0.6872, 0.6861, 0.6954, 0.6817]
5	K-nearest	0.6429	0.0059	[0.6509, 0.6356, 0.6476, 0.6432, 0.637]
1	Decision	0.6012	0.0065	[0.6096, 0.6059, 0.5939, 0.6034, 0.5933]

Table ESM 3. Classification report of the SVC ML model with ^{13}C NMR data of human dopamine D1 receptor antagonists.

	precision	recall	f1-score	support
Active (target 1)	0.68	0.82	0.74	2733
Inactive (target 0)	0.77	0.61	0.68	2733
accuracy			0.71	5466
macro avg	0.73	0.71	0.71	5466
weighted avg	0.73	0.71	0.71	5466

Table ESM 4. Results of ML with ¹³C NMR data of human dopamine D1 receptor antagonists reduced by PCA.

1.Algorithm	2.Accuracy	3.Precision	4.Recall	5.F1	6.ROC
SVM	0.642	0.696	0.506	0.586	0.642
RandomForest	0.619	0.704	0.411	0.519	0.619
GradientBoost	0.619	0.645	0.530	0.582	0.619
XGBoost	0.615	0.659	0.478	0.554	0.615
K-nearest	0.580	0.612	0.438	0.511	0.580
Decision	0.544	0.555	0.444	0.493	0.544

Table ESM 5. Five-fold cross-validation results of ML with ¹³CNMR data of human dopamine D1 receptor antagonists reduced by PCA.

1.Algorithm	2.Mean CV Score	3.Standard Deviation	4.List of CV Scores
SVM	0.6830	0.0052	[0.6881, 0.6808, 0.6782, 0.6903, 0.6778]
RandomForest	0.6713	0.0072	[0.6736, 0.6601, 0.6753, 0.6809, 0.6667]
GradientBoost	0.6663	0.0074	[0.6775, 0.659, 0.6654, 0.6718, 0.6581]
XGBoost	0.6616	0.0040	[0.6676, 0.6595, 0.6561, 0.6645, 0.6604]
K-nearest	0.6205	0.0043	[0.6239, 0.6147, 0.6158, 0.6239, 0.6242]
Decision	0.5780	0.0094	[0.5878, 0.5752, 0.5856, 0.5801, 0.5615]

Table ESM 6. Classification report of the SVC ML model with ¹³CNMR data of human dopamine D1 receptor antagonists reduced by PCA.

	precision	recall	f1-score	support
Active (target 1)	0.61	0.78	0.69	2733
Inactive (target 0)	0.70	0.51	0.59	2733
accuracy			0.64	5466
macro avg	0.65	0.64	0.64	5466
weighted avg	0.65	0.64	0.64	5466

Table ESM 7. Results of CID_SID ML models with ¹³C NMR data of human dopamine D1 receptor antagonists.

1.Algorithm	2.Accuracy	3.Precision	4.Recall	5.F1	6.ROC
XGBoost	0.802	0.863	0.704	0.776	0.799
GradientBoost	0.801	0.885	0.677	0.767	0.797
RandomForest	0.790	0.812	0.738	0.774	0.789
K-nearest	0.774	0.784	0.738	0.761	0.773
SVM	0.766	0.827	0.655	0.731	0.763
Decision	0.757	0.748	0.752	0.750	0.756

Table ESM 8. Five-fold cross-validation results of the CID_SID ML models with ¹³CNMR data of human dopamine D1 receptor antagonists.

1.Algorithm	2.Mean CV Score	3.Standard Deviation	4.List of CV Scores
XGBoost	0.8071	0.0047	[0.8133, 0.7995, 0.8084, 0.8097, 0.8046]
GradientBoost	0.8031	0.0038	[0.8052, 0.7991, 0.8092, 0.7997, 0.8022]
RandomForest	0.7903	0.0059	[0.7957, 0.7813, 0.7957, 0.7938, 0.7853]
K-nearest	0.7810	0.0036	[0.7811, 0.7745, 0.783, 0.7853, 0.7811]
Decision	0.7524	0.0090	[0.7648, 0.7457, 0.7578, 0.7546, 0.7394]
SVM	0.7439	0.0032	[0.7434, 0.7425, 0.7502, 0.7427, 0.7408]

Table ESM 9. Classification report of the XGBC CID_SID ML mode with ¹³CNMR data of human dopamine D1 receptor antagonists.

	precision	recall	f1-score	support
Active (target 1)	0.76	0.90	0.82	2430
Inactive (target 0)	0.87	0.70	0.78	2293
accuracy			0.80	4723
macro avg	0.81	0.80	0.80	4723
weighted avg	0.81	0.80	0.80	4723

2. Figures

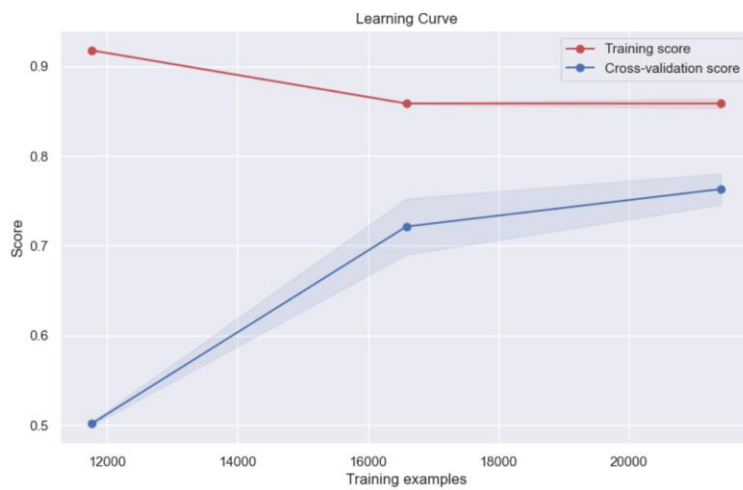


Fig. ESM 1. Learning curve off ML with ¹³CNMR data of human dopamine D1 receptor antagonists

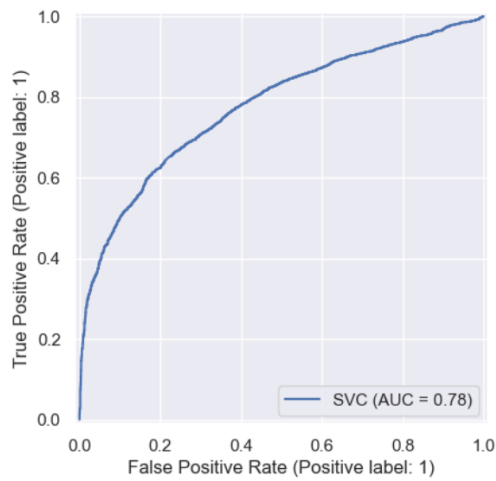


Fig. ESM 2. ROC curve of ML with ¹³CNMR data of human dopamine D1 receptor antagonists

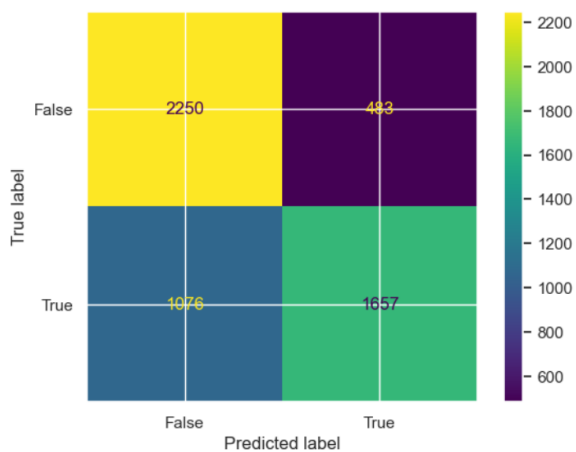


Fig. ESM 3. Matrix off ML with ¹³CNMR data of human dopamine D1 receptor antagonists

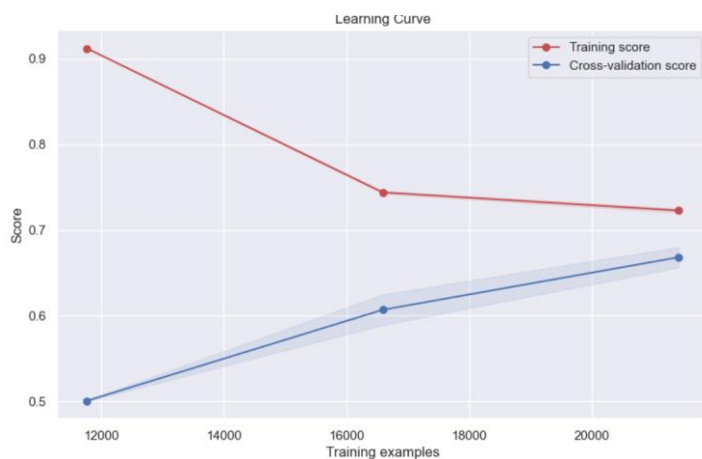


Fig. ESM 4. Learning curve off ML with ^{13}C NMR data of human dopamine D1 receptor antagonists reduced by PCA

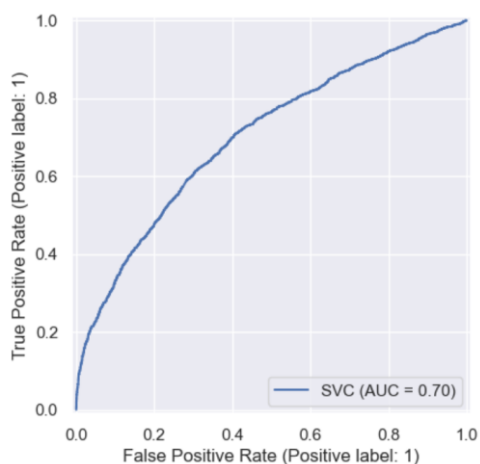


Fig. ESM 5. ROC curve of ML with ^{13}C NMR data of human dopamine D1 receptor antagonists reduced by PCA

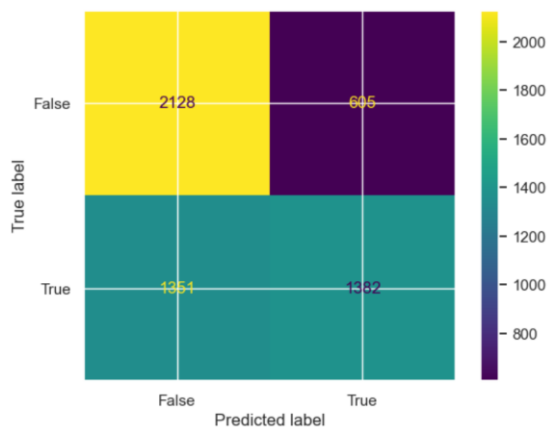


Fig. ESM 6. Matrix off ML with ^{13}C NMR data of human dopamine D1 receptor antagonists reduced by PCA

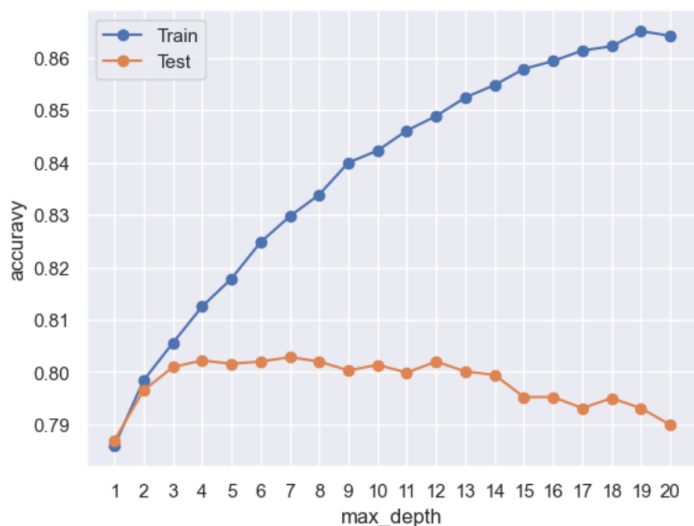


Fig. ESM 7. Tracing the deviation between train and test accuracy of the XGBC CID_SID ML model with 13CNMR data of human dopamine D1 receptor antagonists

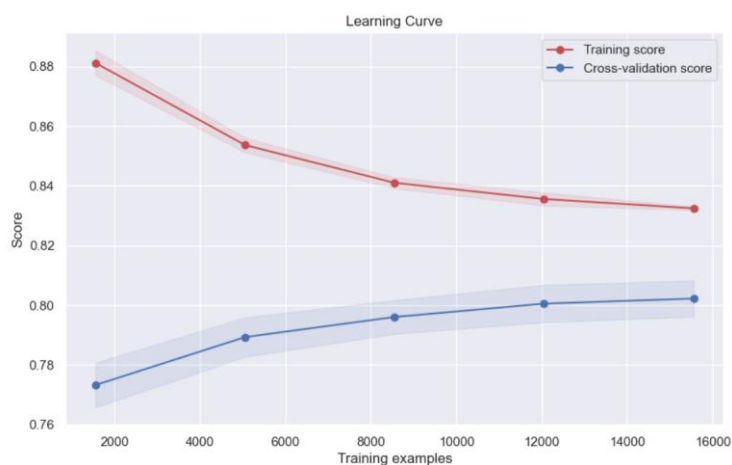


Fig. ESM 8. Learning curve of the XGBC CID_SID ML model with 13CNMR data of human dopamine D1 receptor antagonists

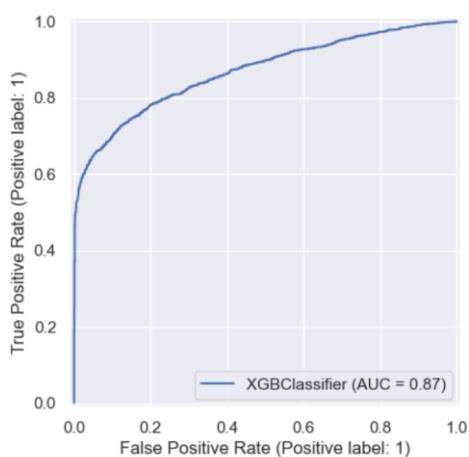


Fig. ESM 9. ROC curve of the XGBC CID_SID ML model with 13CNMR data of human dopamine D1 receptor antagonists

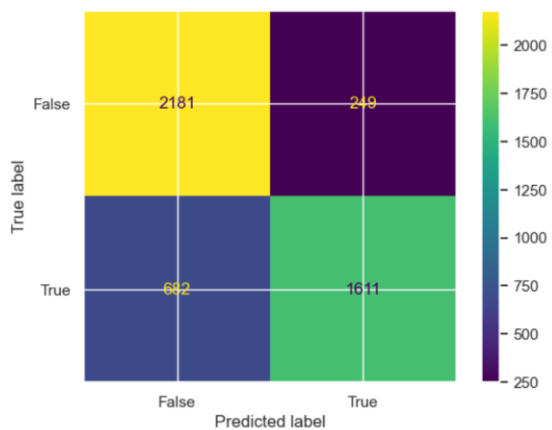


Fig. ESM 10. Matrix of the XGBC CID_SID ML model with ¹³CNMR data of human dopamine D1 receptor antagonists